

Electromagnetic Filters Based on a Single Negative Photonic Comb-Like Structure

Youssef Ben-Ali¹, Zakaria Tahri^{1, 2}, and Driss Bria^{1, *}

Abstract—This work describes a theoretical study of filters using a defect in one-dimensional photonic comb-like structure. This photonic comb-like structure is constituted by finite or infinite segments which have negative permeability and grafted in each site by a finite number of lateral branches (play the role of the resonators), which consists of a negative permittivity. Numerical results exhibit the permissible bands which are separated by gaps (forbidden band). These gaps originate not only from the periodicity of the system but also from the resonance states of the grafted lateral branches. We study the effect of the presence of a resonator defect on the transmission behavior, phase, and phase time. The electromagnetic band structure shows that there is a defect mode in the gap. The transmission rate and the reduced frequency of this mode are related to the variation of defect length. Similarly, we calculate, for the first time, the quality factor evolution of this defect mode when the defect length varies. This structure can be used as a new optical filter in the microwave range with a high factor of quality and of transmission.

1. INTRODUCTION

Left-handed material (LHM), in which the electric permittivity ε and magnetic permeability μ are simultaneously negative at certain frequencies, has attracted tremendous attention in scientific and engineering communities [1–3]. These materials provide numerous unusual properties and phenomena because of their special interaction with incident radiation, which are applied to some important fields [4–9]. Recently, the tunneling of light through single negative (SNG) meta-materials has attracted a lot of attention because of their importance in different fields [10–15]. These mediums (SNG) are experimentally realized in previous studies [16–18]. For example, many plasmas (such as noble metals including gold and silver in infrared and visible regions) which exhibit the electric negative characteristic or gyrotropic (gyromagnetic) materials (such as ferromagnetic materials) show magnetic negative characteristic. Therefore, particular efforts have been purposed in exploring how some of the exciting phenomena and applications predicted and studied in (LHMs) can be transferred into SNGs [19–21]. In general, there are two types of SNG materials. The first one, called the epsilon-negative (ENG) material, which has a negative real part of the complex permittivity and a positive real permeability ($\varepsilon < 0$ and $\mu > 0$). The second one, called the mu-negative (MNG) materials, has a negative real part of the complex permeability and a positive real permittivity ($\varepsilon > 0$ and $\mu < 0$) [22–24].

Three previous papers [25–27] proposed a model of a one-dimensional (1D) photonic comb-like structure (also called star waveguide) exhibiting electromagnetic bands separated by large gaps (zeros of transmission). This system is composed by an infinite 1D segment (the backbone) along which a finite site of resonators are grafted periodically. The gaps originate both from the periodicity of the system and the resonance states of resonators [28], and these gaps occur at particular frequencies

Received 20 December 2018, Accepted 25 March 2019, Scheduled 19 April 2019

* Corresponding author: Driss Bria (drissbria@gmail.com).

¹ Laboratoire de Dynamiques et d’Optiques de Matériaux, Faculté de Science, Université Mohamed Premier, Oujda 60000, Maroc.

² Ecole National des Sciences Appliquées, Université Abdelmalek Essaâdi, Al Hoceima, Maroc.

related to the length and physical characteristics of the side branch. These frequencies are broadened into gaps when several side branches are grafted at equidistant nodes along the waveguide. Using these gaps, the electromagnetic waves can be controlled and manipulated effectively, so gaps materials have been found to have a wider range of applications [25–28]. When left-handed materials are introduced into these systems, some unusual band gaps can also be found [29–32]. Recently, a metallic comb-like waveguide structure was studied, showing the possibility of achieving high transmission through negative-permittivity chain with the scale of a wavelength [33]. Another work manages to achieve complete tunneling through MNG media by using the comb-like structure [34]. A defect is one of the elements for which the star waveguide structure is developed and can filter a given frequency very effectively out of different frequencies. In our recent work, we show for the first time that the presence of a resonator defect in the LHM comb-like structure can give rise to localized states (defect modes) inside the band gaps. These states are very sensitive to the defect length, number of sites, position of defect, and number of defective resonators [35]. These defect modes can be used to design filters, demultiplexing, etc. [28].

In this work, we show that a one-dimensional photonic comb-like structure (the segment constituted by an MNG material and the resonator constituted by a material ENG) which contains a finite number N'_0 of resonators defect can be used as a filter for application in telecommunication field [36]. The purpose of this paper is to calculate for the first time the evolution of the quality factor Q (the ratio of the central frequency and the full width at half-maximum of the transmittance modes) of defect modes in the photonic comb-like structure which contains ENG and MNG materials. It is worth pointing out again the conditions of validity of the model. In all our calculations we have assumed that the cross section of the segment is small compared to its linear dimension, that is, the segment may be considered as a one-dimensional medium.

2. MODEL AND FORMALISM

2.1. Dispersion Relation through an Infinite Photonic Comb-Like Structure

We consider the structure (Fig. 1(a)) which consists of infinity of segments of length d_1 along the direction x . The position x in a cell between the sites n and $n + 1$ is represented by the pair (n, x) where x is a local coordinate such that $0 \leq x \leq d_1$. To calculate the Green function of the infinite structure, we need to determine the elements of the function g_{si}^{-1} of a segment ($i = 1$) of length d_1 in each cell (n, x) for any n such that $-\infty \leq n \leq +\infty$ and the Green function of a length resonator d_2 ($i = 2$) in

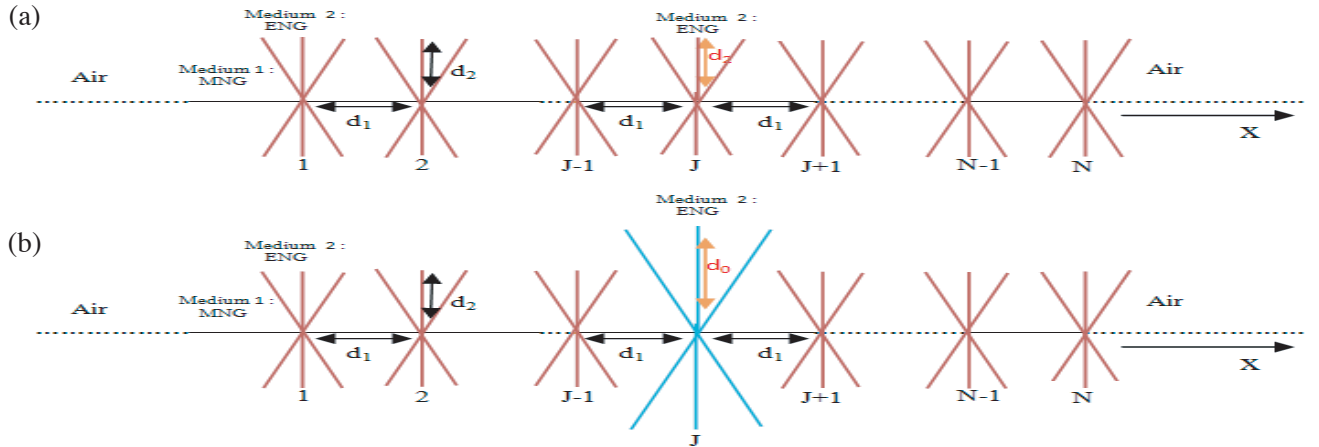


Figure 1. (a) One-dimensional photonic comb-like filter constituted by a periodicity of MNG segment of length d_1 , grafted in each site N by a finite number of ENG lateral branches of length d_2 with $N' = 6$. (b) Same as (a) except that there is a defect at the side branch at site J of the length d_0 with the defect lateral branch number is $N'_0 = 6$. The segment and the side branches (resonators) are constituted by the coaxial cables (transmission lines) [25].

each site n . These surface elements are denoted respectively $g_{s1}^{-1}(M_1; M_1)$, which are a matrix $(2 * 2)$ in the interface space $M_1 = \{0; d_1\}$ and the element $g_{s2}(0; 0) = g_{s2}(d_1; d_1)$.

The inverse matrix of the one segment located between the space $\{0; d_1\}$ is given in [25]:

$$\overleftrightarrow{g_{si}^{-1}}(M_i M_i) = \begin{pmatrix} -\frac{F_i C_i}{S_i} & \frac{F_i}{S_i} \\ \frac{F_i}{S_i} & -\frac{F_i C_i}{S_i} \end{pmatrix} \quad (1)$$

while $g_{s2}(0; 0) = g_{s2}(d_1; d_1)$ depends on the choice of the boundary conditions on the end of the branches, for the case where $H = 0$. This quantity is given by:

$$g_{s2}^{-1}(0, 0) = -\frac{S_2 F_2}{C_2} \quad (2a)$$

with:

$$C_i = \cosh(\alpha_i d_i) \quad \text{and} \quad S_i = \sinh(\alpha_i d_i) \quad (2b)$$

$$\alpha_i = j \frac{\omega}{c} \sqrt{\epsilon_i \mu_i} \quad (2c)$$

$$F_i = \frac{\alpha_i}{\mu_i} \quad (2d)$$

$$j = \sqrt{-1} \quad (2e)$$

In the interface space of the infinite comb structure, the inverse of the matrix of the Green function $\overleftrightarrow{g_{\infty}^{-1}}(M_i M_i)$ is an infinite tridiagonal matrix formed by the superposition of the elements $\overleftrightarrow{g_{si}^{-1}}(M_i M_i)$ ($i = 1; 2$). This matrix is written as follows:

$$\overleftrightarrow{g_{\infty}^{-1}}(M_i M_i) = \begin{pmatrix} \ddots & \ddots & \ddots & & \\ v & w & v & & \\ & v & w & v & \\ & & v & w & \\ & & & \ddots & \ddots \end{pmatrix} \quad (3a)$$

with:

$$v = \frac{F}{S} \quad (3b)$$

$$w = -2F_1 \frac{C_1}{S_1} - N' \frac{S_2 F_2}{C_2} \quad (3c)$$

Using the theorem of the Bloch, we deduce the dispersion relation in the form:

$$-2F_1 \frac{C_1}{S_1} - N' \frac{S_2 F_2}{C_2} + \frac{F_1}{S_1} (e^{jkd_1} + e^{-jkd_1}) = 0 \quad (4a)$$

from where:

$$\cos(kd_1) = C_1 + \frac{1}{2} S_1 S_2 \frac{N' F_2}{F_1 C_2} \quad (4b)$$

The system is periodic in the direction x , and the Fourier transform $\overleftrightarrow{g^{-1}}[(k; M; M)]$ of the infinite tridiagonal matrix in a segment of length d_1 is written as follows:

$$\overleftrightarrow{g^{-1}}[(k; M; M)] = -2F_1 \frac{C_1}{S_1} - N' \frac{S_2 F_2}{C_2} + \frac{F_1}{S_1} (e^{jkd_1} + e^{-jkd_1}) \quad (5a)$$

where k is the reciprocal wave vector.

From where:

$$\overleftrightarrow{g^{-1}}[(k; M; M)] = 2 \frac{F_1}{S_1} [-\eta + \cos(kd_1)] \quad (5b)$$

with η is given by:

$$\eta = C_1 + \frac{1}{2}S_1S_2\frac{N'F_2}{F_1C_2} \quad (5c)$$

The bulk bands of the comb-like structure are obtained from the poles of the Green function by the following relation:

$$\cos(kd_1) = \eta \quad (6)$$

The inverse Fourier transform of $\overleftrightarrow{g}[(k; M; M)]$ is given by:

$$\overleftrightarrow{g}[(n, n')] = \frac{S_1 t^{|n-n'|+1}}{F_1 t^2 - 1} \quad (7a)$$

where the integers n and n' represent the sites on the infinite comb-like ($-\infty \leq n, n' \leq +\infty$), and parameter t is given by [25]:

$$t = e^{jkd_1} \quad (7b)$$

2.2. Coefficient of Transmission through a Finite Comb-Like Structure

In this section, we consider the quasi-one-dimensional photonic comb-like structure. This composite system is constructed out of a finite comb-like structure cut out of the infinite periodic system of Fig. 1(a), which is subsequently connected at its extremities to two semi-infinite leading lines. The finite comb-like structure is therefore composed of N resonators (medium 2) of length d_2 grafted periodically with a lattice spacing d_1 on a finite line (medium 1). For the sake of simplicity, the semi-infinite leads are assumed to be constituted of the same material as medium 1. The system of Fig. 1(b) is constructed from the infinite comb-like structure (Fig. 1(a)). In the first step, one suppresses the segments linking sites $n = -1$ and $n = 0$, and sites $n = N$ and $n = N + 1$. In the second step, a defect is created inside the structure by a change of a lateral branch of length d_2 , permittivity ε_2 , and permeability μ_2 located at site J by another resonator of length d_0 , permittivity $\varepsilon_0 = \varepsilon_2$, and permeability $\mu_0 = \mu_2$. The disturbance states are $M_s = \{-1, 0, J, N, N + 1\}$.

The inverse surface Green's function $\overleftrightarrow{g}_t^{-1}(M_s M_s)$ of the structure comb-like structure containing a defect for the condition $H = 0$ is the following $5 * 5$ square matrix defined in the interface domain constituted in sites $-1, 0, J, N, N + 1$.

$$\overleftrightarrow{g}_t^{-1}(M_s M_s) = \begin{pmatrix} A & 0 & 0 & 0 & 0 \\ 0 & B & 0 & 0 & 0 \\ 0 & 0 & C & 0 & 0 \\ 0 & 0 & 0 & D & 0 \\ 0 & 0 & 0 & 0 & D \end{pmatrix} \quad (8a)$$

with:

$$A = -N'\frac{F_2S_2}{C_2} - \frac{F_1C_1}{S_1}, \quad B = -\frac{F_1C_1}{S_1}, \quad C = N'_0\frac{F_0S_0}{C_0} \quad \text{and} \quad D = -N'\frac{F_2S_2}{C_2} - \frac{F_1C_1}{S_1} \quad (8b)$$

The cleavage operator $\overleftrightarrow{V}(M_s M_s) = \overleftrightarrow{g}_t^{-1}(M_s M_s) - \overleftrightarrow{g}_\infty^{-1}(M_s M_s)$ is the following $4 * 4$ square matrix defined in the interface domain constituted of sites $-1, 0, J, N, N + 1$:

$$\overleftrightarrow{V}(M_s M_s) = \begin{pmatrix} E & F & 0 & 0 & 0 \\ F & G & 0 & 0 & 0 \\ 0 & 0 & H & 0 & 0 \\ 0 & 0 & 0 & E & F \\ 0 & 0 & 0 & F & E \end{pmatrix} \quad (9a)$$

with:

$$E = \frac{F_1C_1}{S_1}, \quad F = -\frac{F_1}{S_1}, \quad G = \frac{F_1C_1}{S_1} + N'\frac{F_2S_2}{C_2} \quad \text{and} \quad H = N'\frac{F_2S_2}{C_2} - N'_0\frac{F_0S_0}{C_0} \quad (9b)$$

Or: $\overleftrightarrow{g}_\infty^{-1}(M_s M_s)$ is the inverse Green function of the infinite system (see Equation (3a)).

The knowledge of the elements of the response function in the interface space of the infinite comb-like structure $\overleftarrow{g}_\infty^{-1}(M_s M_s)$ and those of the cleavage operator $\overleftrightarrow{V}(M_s M_s)$ allow us to deduce the elements of the response function of the finite structure necessary for the calculation of the transmission coefficient.

The surface response operator $\overleftrightarrow{A}(M_s M_s)$ is written as follows:

$$\overleftrightarrow{A}(M_s M_s) = \sum_{M_s} \overleftrightarrow{V}(M_s M_s) \overleftarrow{g}(M_s M_s) \quad (10)$$

The function $\overleftarrow{g}(M_s M_s)$ is computed from Equation (7a):

$$\overleftarrow{g}(M_s M_s) = \frac{S_1}{F_1} \frac{t}{t^2 - 1} \begin{pmatrix} 1 & t & t^{J+1} & t^{N+1} & t^{N+2} \\ t & 1 & t^J & t^N & t^{N+1} \\ t^{J+1} & t^J & 1 & t^{N-J} & t^{N+1-J} \\ t^{N+1} & t^N & t^{N-J} & 1 & t \\ t^{N+2} & t^{N+1} & t^{N+1-J} & t & 1 \end{pmatrix} \quad (11)$$

The parameter t is given in Equation (7b)

The operator $\overleftrightarrow{\Delta}(M_s M_s)$ is given by the following relation:

$$\overleftrightarrow{\Delta}(M_s M_s) = I(M_s M_s) + \overleftrightarrow{A}(M_s M_s) \quad (12)$$

After calculating the operator $\overleftrightarrow{\Delta}(M_s M_s)$, let us write this operator in space $M_0 = \{0, J, N\}$.

$$\begin{aligned} & \overleftrightarrow{\Delta}(M_0 M_0) \\ &= \begin{pmatrix} 1 + \sigma \left(\frac{F_1 C_1}{S_1} + N' \frac{F_2 S_2}{C_2} + -\frac{F_1 t}{S_1} \right) & \sigma t^J \left(\frac{F_1 C_1}{S_1} + N' \frac{F_2 S_2}{C_2} + -\frac{F_1 t}{S_1} \right) & \sigma t^N \left(\frac{F_1 C_1}{S_1} + N' \frac{F_2 S_2}{C_2} + -\frac{F_1 t}{S_1} \right) \\ \sigma t^J \left(N' \frac{F_2 S_2}{C_2} - N'_0 \frac{F_0 S_0}{C_0} \right) & \sigma t \left(N' \frac{F_2 S_2}{C_2} - N'_0 \frac{F_0 S_0}{C_0} \right) + 1 & \sigma t \left(N' \frac{F_2 S_2}{C_2} - N'_0 \frac{F_0 S_0}{C_0} \right) t^{N-J} \\ \sigma t^N \left(-\frac{F_1 t}{S_1} + \frac{F_1 C_1}{S_1} \right) & \sigma t^{N-J} \left(-\frac{F_1 t}{S_1} + \frac{F_1 C_1}{S_1} \right) & 1 + \sigma \left(-\frac{F_1 t}{S_1} + \frac{F_1 C_1}{S_1} \right) \end{pmatrix} \end{aligned} \quad (13a)$$

with

$$\sigma = \frac{S_1}{F_1} \frac{t}{t^2 - 1} \quad (13b)$$

The Green function of surface $\overleftrightarrow{d}(M_0 M_0)$ for a finite comb-like structure is defined in space M_0 by the following equation:

$$\overleftrightarrow{d}(M_0 M_0) = \overleftarrow{g}(M_0 M_0) \overleftrightarrow{\Delta}^{-1}(M_0 M_0) \quad (14)$$

with $\overleftrightarrow{\Delta}^{-1}(M_0 M_0)$ being the inverse of the operator $\overleftrightarrow{\Delta}(M_0 M_0)$.

We deduce the truncated matrix $\overleftrightarrow{d}_{tr}(M_0 M_0)$ in the space $M'_0 = \{0, N\}$. The inverse of this matrix is written in the form:

$$\overleftrightarrow{d}_{tr}^{-1}(M'_0 M'_0) = \begin{bmatrix} A_{11} & A_{12} \\ A_{21} & A_{22} \end{bmatrix} \quad (15)$$

where elements A_{11}, A_{12}, A_{21} , and A_{22} are, respectively, (1,1), (1,3), (3,1), and (3,3) elements of the inverse matrix of $\overleftrightarrow{d}(M_0 M_0)$.

Finally, the Green function of a finite photonic comb-like structure $\overleftrightarrow{d}_h^{-1}(M'_0 M'_0)$ located between two semi-infinite media is:

$$\overleftrightarrow{d}_h^{-1}(M'_0 M'_0) = \begin{bmatrix} A_{11} - F_1 & A_{12} \\ A_{21} & A_{22} - F_1 \end{bmatrix} \quad (16a)$$

with F_1 being the Green function of the semi-infinite medium.

Then

$$\overleftrightarrow{d}_h (M'_0 M'_0) = \frac{1}{(A_{11} - F_1)(A_2 - F_1) - A_{21}A_{12}} \begin{bmatrix} A_{22} - F_1 & -A_{21} \\ -A_{12} & A_{11} - F_1 \end{bmatrix} \quad (16b)$$

The transmission coefficient through the structure is given by the following relation [25]:

$$T = -2F_1 \overleftrightarrow{d}_h (s, e) = 2F_1 \frac{1}{(A_{11} - F_1)(A_{22} - F_1) - A_{21}A_{12}} A_{12} \quad (17)$$

with e : The interface between the first substrate (Medium 1) and photonic comb-like structure.

s : The interface between the second substrate 2 (Medium 1) and photonic comb-like structure.

The transmission coefficient can be written in an explicit complex form as:

$$T = \alpha + j\beta = |T| e^{j\varphi} \quad (18)$$

where α is the real part of the transmission, β the imaginary part, $|T|$ the amplitude of the transmission coefficient, and $\varphi = \arctan(\beta/\alpha)$ the phase of transmission. The first derivative of φ with respect to the pulsation represents the time taken by the wave to cross the structure before being transmitted. This quantity is called phase time τ and defined by:

$$\tau = \frac{d\varphi}{d\omega} \quad (19)$$

Let us notice that our numerical calculations are done with the help of the FORTRAN compiler. Equation (1) up to Equation (13b) are analytically obtained; however, we have numerically calculated $\overleftrightarrow{d} (M_0 M_0)$ matrix, given by Equation (14). The last one is the product of the two matrices $\overleftrightarrow{g} (M_0 M_0)$ and $\overleftrightarrow{\Delta}^{-1} (M_0 M_0)$. Numerically, we truncate the matrix $\overleftrightarrow{d} (M_0 M_0)$ in matrix $(2 * 2)$, and we limit our structure by two semi-infinite media. Finally, we numerically deduce the relation of transmission coefficient of Eq. (17), which allows us to determine the phase in Eq. (18) and the phase time in Eq. (19).

3. RESULTS AND DISCUSSIONS

In this work, we study the effect of the introduction of a defect at the resonator level on 1D photonic comb-like structure (see Figure 1(b)). In our calculations, we illustrate the electromagnetic band structure, transmission coefficient, phase, and phase time for a comb-like structure. This structure is constituted by resonators which have a permittivity dielectric $\varepsilon_2(\omega) = 1 - \frac{1.33^2}{\Omega^2}$ dependent on the frequency and a positive magnetic permeability $\mu_2 = 1$. So, the segment is constituted by a positive dielectric $\varepsilon_1 = 2$, and the magnetic permeability $\mu_1(\omega) = 1 - \frac{1.33^2}{\Omega^2}$ is dependent on the frequency [34]. The segment length is d_1 , and the resonator length is d_2 with $D = d_1$ being the period of the structure. The dielectric and magnetic characteristics of the defect are the same as that for the resonator, but the length is denoted as d_0 which is different from d_2 , and the number of defect resonators grafted is noted by N'_0 .

We investigate and discuss the structure of the band gap with the various parameters of length d_0 , of the number of defective resonators N'_0 and the number of sites N . The reduced frequency is $\Omega = \omega\sqrt{(\varepsilon_1)d_1}/(c)$, with c being the speed of light and ω the frequency (s^{-1}).

We focus our attention on the frequency regions where the permeability $\mu_1(\omega)$ of the MNG media and the permittivity $\varepsilon_2(\omega)$ of the ENG media are simultaneously negative, which is when Ω is varied from 0 to 1.33.

3.1. Confined Modes of a Single Resonator

Now, we are interested in the confined modes (branches) of a single ENG resonator of medium 2 of length d_2 , extending in the region $x_3 = 0$, embedded between two semi-infinite RHMs made of material 1 (Air). Fig. 2(a) represents the variation of reduced frequency of the single resonator versus length d_2 . We note from this figure that the branches of a single resonator are decreased in frequency with the increase of resonator length d_2 , and these branches have a cutoff frequency where their propagation is impossible below this cutoff frequency. The appearance of these branches, which is very sensitive

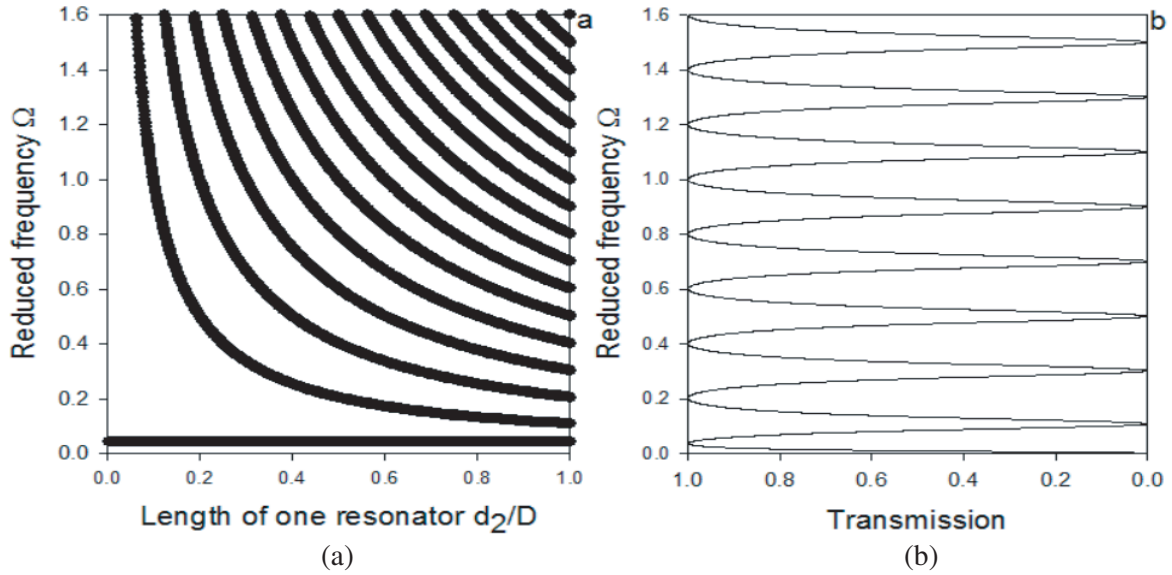


Figure 2. (a) represents the reduced frequency Ω versus the length of one resonator d_2 . (b) represents the transmission coefficient versus the reduced frequency Ω for $d_2 = 1D$.

to the length d_2 , is due to the interaction between the modes of a single resonator and the waveguide input. So, we deduce that the periodicity of the structure comes from the interaction of the modes of each resonator with the other neighbors. Fig. 2(b) shows the variation of the transmission as a function of the reduced frequency Ω for the single resonator length $d_2 = 1D$. These curves present minima (transmission zero) and maxima transmissions. The phenomenon of transmission zero is related to the resonances associated with the finite additional path offered to the electromagnetic wave propagation. The frequencies corresponding to the maxima of these curves give the modes (discrete modes) of the single resonator. This result is similar to that found by Vasseur et al. except that they used right-handed materials [25]. The modes of the single resonator are very wide (their quality factor is very low), hence, we need to study a periodic structure containing several resonators.

3.2. Electromagnetic Band Structure of a Perfect Comb-Like Structure

In this section, we analyze and compare properties of the band structure and the transmission coefficient for a perfect comb-like structure without defect when $d_0 = d_2$, $N = 8$, $N' = N'_0 = 1$, $d_1 = 1D$, and $d_2 = 0.5D$. Fig. 3(a) shows the first three dispersion curves (black lines) in the band structure of an infinite comb-like structure. One can observe a first gap (gap is located in the white regions and between two red lines) before the first passband (regions where there are black lines), the second gap between the first and the second passbands, the third gap between the second and third passbands, and another gap after the third passband. The real part of the reduced wave vector (kd_1) is in very good agreement with the transmission through a finite sized comb-like structure (Fig. 3(b)). The latter originates both from the periodicity of the structure, related to the length d_1 , and from the resonant behavior of the lateral branches, related to the length d_2 . In particular, the resonators give rise to zeros of transmission through the waveguide at frequencies such that $\cos(\omega d_2 \sqrt{\epsilon_1}/c)$ [27]. Fig. 3(c) indicates the variation of the phase versus the reduced frequency Ω . One can notice that the phase increases monotonically almost of π in band gap. Fig. 3(d) shows the variation of the phase time versus the reduced frequency Ω . We note in Fig. 3(d) that the phase time of a few discrete modes is very high. We also observe that there are four gaps; the gaps are seen as zero transmission ranges in the transmission coefficient.

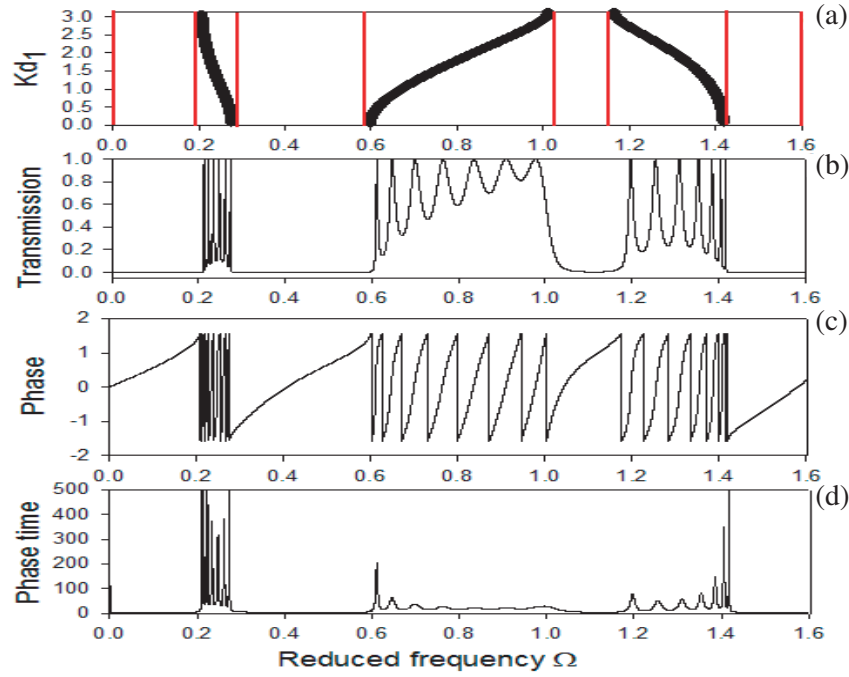


Figure 3. (a) Band structure of the infinite comb-like structure (reduced frequency Ω as a function of the reduced Bloch wave vector kd_1). (b) The transmission spectrum through a finite comb-like structure. (c) and (d) respectively are the phase and phase time spectrum in the same situation of the curve (b).

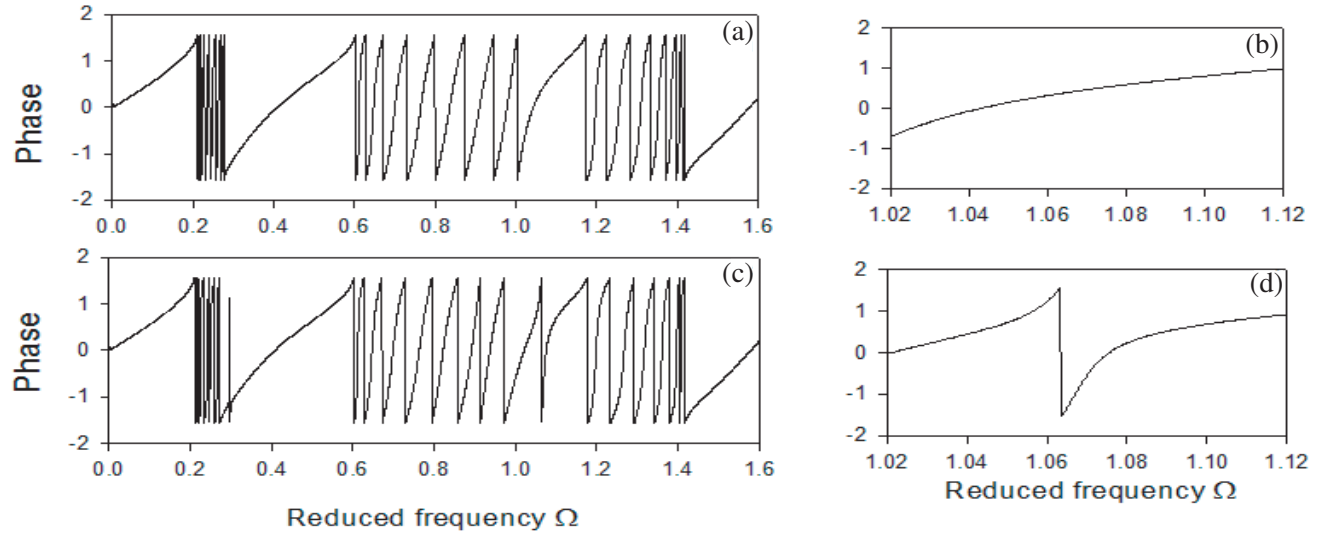


Figure 4. (a) shows the phase as function of reduced frequency Ω without defect, (b) is a curve zoom of (a). (c) shows the phase as a function of reduced frequency Ω with the presence of defect, (d) is a zoom of (c).

3.3. Effect of Defect on the Phase

In this subsection, we briefly study the effect of the presence of the defect on the phase behavior with $J = 5$, $N' = N'_0 = 1$, $N = 8$, $d_1 = 1D$, and $d_2 = 0.5D$. Fig. 4 shows the variation of the phase versus the reduced frequency. One can notice that when there is no defect in the structure (Fig. 4(a)), the phase increases monotonically in the band gap (this result is very clear in Fig. 4(b), but when a defect

is introduced into the structure with $d_0 = 2d_2$, the phase exhibits a jump of π around the position of the defect mode then a fall of $-\pi$ due to the transmission zero (Fig. 4(d)).

3.4. Transmission and Phase Time as a Function of the Parameter N

The introduction of a defect inside a perfect star waveguide structure leads to confined resonance modes (defect modes) owing to the change of the interference behavior of electromagnetic EM waves, whose frequencies depend on both the relative permittivity and/or the length of the defect. In this section, we study the transmission spectrum and phase time of the defect modes versus reduced frequency Ω for different values of N with $N' = N'_0 = 1$, $J = 5$, $d_0 = 2d_2$, $d_1 = 1D$, and $d_2 = 0.5D$. The results of transmission are presented in the left of Fig. 5, and the result of phase time variation is represented in the right of Fig. 5 for three different values of N , namely $N = 8$ (a), $N = 10$ (b), and $N = 14$ (c). For case (a) when $N = 8$, we observe that there is a defect mode in the second gap with a small transmission, and another mode is in the third gap with a high transmission, so we note the absence of the defect modes in the first and fourth gaps. According to the left panel, one can notice that the frequencies of the defect modes are totally independent of N , whereas their intensities of transmission coefficient decrease progressively with increasing N (Fig. 5(c)). This phenomenon (the decrease of the intensities) appears in contradiction with the fact that, by increasing N , the localization degree of these modes around the defect increases, and therefore the peaks associated with the defect modes are narrow (the quality factor of these defect modes increases). However, this behavior can be explained by the loss of the energy of the mode (attenuation of the structure) that leads to a widening of the peaks due to the absorption phenomenon, but also leads to a decrease in the transmitted intensity due to an enhancement of the reflected intensity. Despite this limitation, the transmission peaks of defect modes present an important transmission and very narrow bandwidth, which permits a selective transmission of frequency particularly for $N = 8$ and $N = 10$ (The constructive effect of the electromagnetic wave can explain the reason that the transmission of defect modes is important in these two cases). Similarly, we note that the position of the gaps is independent of the value of N ; this result is different from that found by Wang et al. [37].

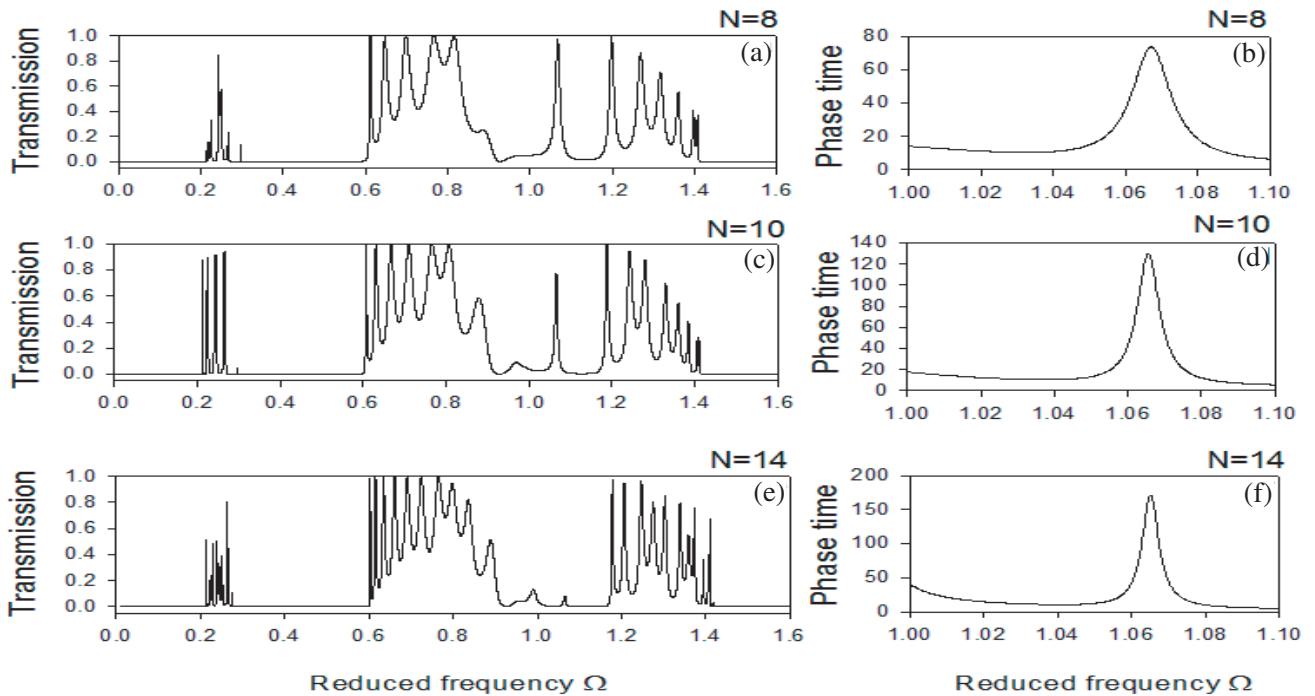


Figure 5. Transmission spectrum (left panel) and phase time (right panel) versus reduced frequency Ω for different values of N , namely (a) $N = 8$, (b) $N = 10$, and (c) $N = 14$.

According to the right panel of Fig. 5, the phase time associated with the defect modes is increased when N increases because the defect modes become more localized, and the trapping time of electromagnetic wave increases (contrary to the amplitude of the defect modes in the transmission spectra of the right panel).

We focus our attention on the high mode located in the third gap.

3.5. Transmission and Phase Time as a Function of the Parameter N'_0

In the present paper, we study the effect of number of defective grafted lateral branches N'_0 on the transmission behavior of defect modes and their phase time with $d_0 = d_2$, $J = 5$, $N = 8$, $d_1 = 1D$ and $d_2 = 0.5D$. The results of transmission are presented in the left panel of Fig. 6, and the result of phase time variation is represented in the right of Fig. 6 for three different values of N'_0 , namely $N'_0 = 1$, $N'_0 = 3$, and $N'_0 = 4$. According to the left panel of Fig. 6, one notices that the transmission factor in the permissible bands is depressed as N'_0 increases, while the transmission of defect modes is almost independent from N'_0 . Furthermore, we note that the defect modes move towards high frequency when N'_0 increases. Similarly, we observe that the defect modes become narrower with the increase of N'_0 . Therefore, it can be deduced that the quality factor Q of these modes increases substantially with the increase of N'_0 (the degree of localization of defect modes around of defect is increased with N'_0). Therefore, we deduce that there is a dependency between the defect modes and the number of resonators defect grafted. The shifting behavior can be explained by the fact that when N'_0 increases, the frequencies of defect modes must increase accordingly to keep the phase unchanged. Correspondingly the value of frequency must be increased. This result is the same as the one founded by Vasseur et al. when they studied right-handed materials [38].

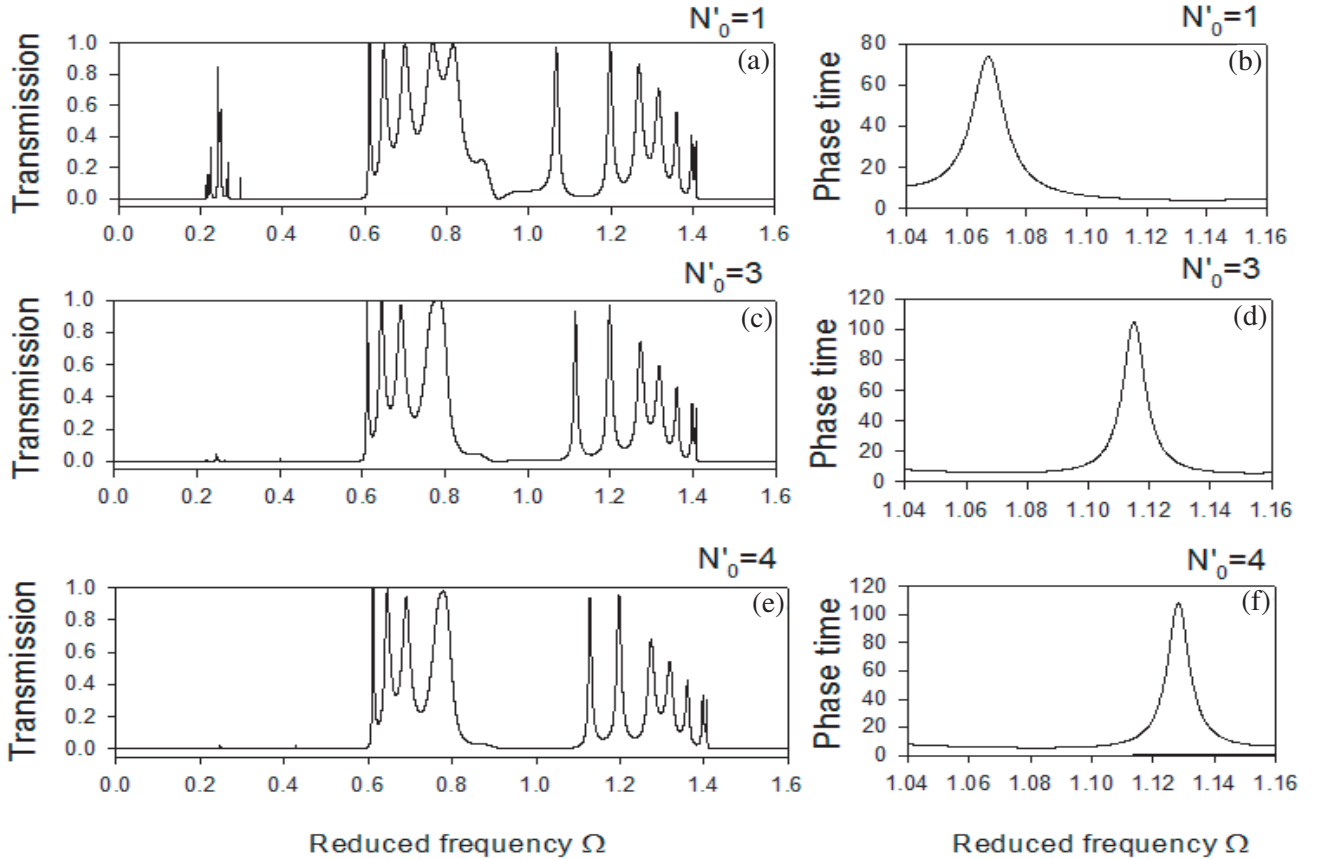


Figure 6. Transmission spectrum (left panel) and phase time (right panel) versus reduced frequency Ω for different values of N'_0 , namely (a) $N'_0 = 1$, (b) $N'_0 = 3$, and (c) $N'_0 = 4$.

As shown in the right panel of Figure 6, it is clearly seen that the phase time intensity of the defect modes is almost constant when $N'_0 = 3$ or 4. This intensity is greater than the intensity when $N'_0 = 1$. The results also show that the phase time quality factor is increased with the increase of N'_0 .

The result of this paragraph will provide theoretical foundation for designing narrow-band filter with high performance.

3.6. Transmission and Phase Time as a Function of the Parameter J

In this part, we study the effect of the defect position variation J inside the structure on the behavior of the transmission of defect modes and their phase time when $d_0 = 2d_2$, $N = 8$, $N' = N'_0 = 1$, $d_1 = 1D$, and $d_2 = 0.5D$. According to the left panel of Fig. 7, one can notice that when the defect is inserted far from the middle of the structure, the amplitude (transmission) of the localized modes decreases progressively. Indeed, the transmission of the defect mode is decreased when the defect lies in the site $J = 5$ (there are four resonators to the left of the defect and three to its right), and practically it vanishes when the defect branch is inserted in the site $J = 7$ (there are six resonators to the left of the defect and one to its right) or $J = 3$ (there are two resonators to the left of the defect and five to its right). This decrease may be explained qualitatively as follows: when the defect is inserted in the middle of the comb-like structure, the structure behaves as two identical segments with $N/2$ resonators connected with a resonator defect. Because of the symmetry of the system, constructive interferences occur and lead to the enhancement of the amplitude of the transmission. However, when the defect branch lies far from the middle of the comb-like structure, the structure behaves as two linked segments with different numbers of resonators. Each of the linked segments contributes in its own way to the transmission of the comb-like. Thus, destructive effects are responsible for the decrease in amplitude when the defect is moved away from the middle of the comb-like structure.

According the right panel of Fig. 7, the same thing happens to the amplitude of the defect modes in the transmission spectra of the left panel of Fig. 7. The phase time and quality factor associated with the defect modes are very high when the defect is located in the middle of the structure ($J = 5$). Indeed, the intensity of the peaks in the phase time is related to the lifetime of the resonances and it reflects the time spent by the electromagnetic wave inside the defect before its transmission. Therefore,

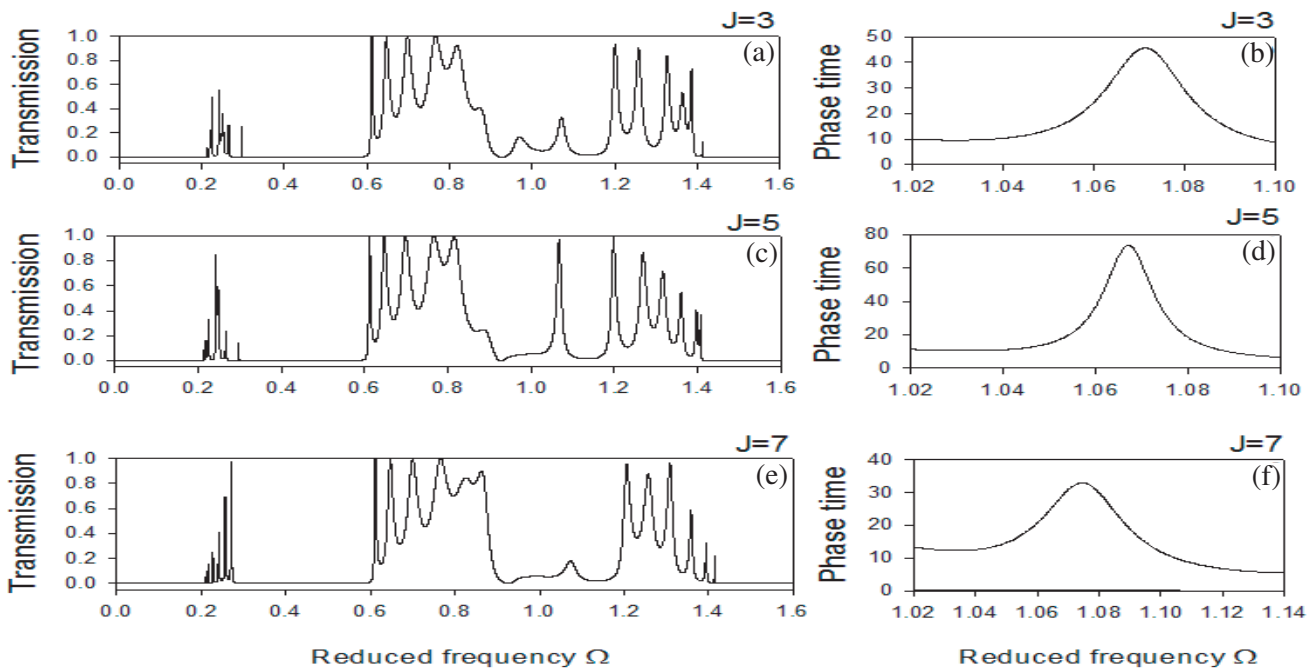


Figure 7. Transmission spectrum (left panel) and phase time (right panel) versus reduced frequency Ω for different values of J , namely (a) $J = 3$, (b) $J = 5$, and (c) $J = 7$.

when the defect is located in the middle, the defect modes overlap around this position, hence these modes have a good quality factor, and the trapping time of electromagnetic wave is high.

The comparison of Figs. 5, 6, and 7 shows that the frequency of the defect mode does not depend on the defect position J and the number of cell N of the structure; however, the frequencies are very sensitive to the number of defective resonators N'_0 . In the rest of this work, we study the influence of the variation of defect length on the behavior of the defect modes.

3.7. Band Structure as a Function of the Parameter d_0/D

In this section, we address the problem of the existence of localized branches of defect and structure in the forbidden bands (gaps) of the photonic structure resulting from the presence of a defect lateral branch inside a comb-like structure. Fig. 8 gives the frequencies of the localized branches versus d_0/D when a defect is introduced into a finite or infinite comb-like structure with $d_1 = 1D$ and $d_2 = 0.5D$. The gray areas represent the perfect infinite comb-like band structure when bulk bands exist (structure branches); these areas are separated by forbidden bands (white areas). The red branches represent the discrete modes of a single resonator; these discrete modes can fall into the forbidden bands or in the bandwidths and can also interact with different branches in the structure. The black branches represent the reduced frequency variation for a finite comb-like structure containing a defect. Firstly, we can see that the branches located in the passbands are varied with length d_0/D . We also note that there are three band gaps with the absence of defect branches in the second band gap which is located between $\Omega = 0.29$ and $\Omega = 0.6$. For the first band gap located between $\Omega = 0$ and $\Omega = 0.2055$ (curve c), we notice that the defect branch increases in frequency with the increase of d_0/D until it becomes a branch of the structure. On the other hand at the third band gap which lies between $\Omega = 1.06$ and $\Omega = 1.163$ (curve b), their reduced frequency Ω is decreased by increasing d_0/D . So, we can deduce that these structures can create defect branches which increase or decrease in frequency by the increase of defect length d_0/D , which is not the case of our previous work [35, 39].

In summary, we can say that we can introduce resonant branches inside a band gap by introducing a geometric defect. We can also define the order of the band gap where we are looking for the defect

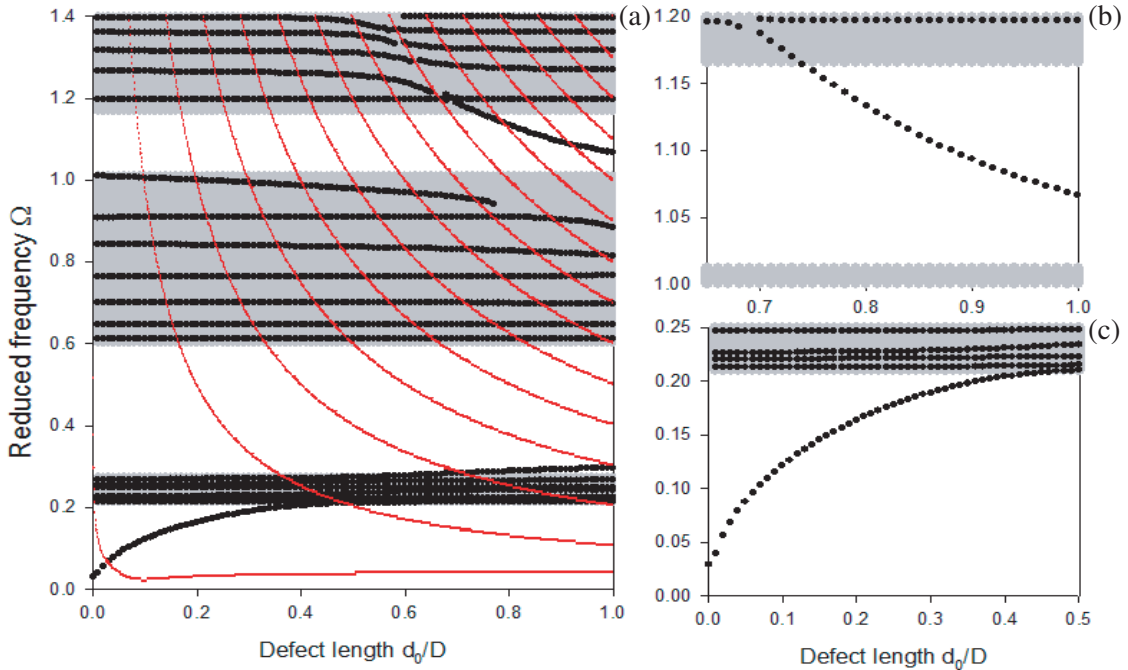


Figure 8. (a) represents the variation of the reduced frequency Ω versus the defect length d_0/D . (b) is the zoom of the area located between $\Omega = 1$ and 1.2. (c) represents the zoom of the area located between $\Omega = 0$ and 0.25.

branches. From a general point of view, to achieve a photonic filter, it is necessary to design a structure in which the transmission coefficient has well-defined characteristics and are very sensitive to electromagnetic waves and relatively isolated to allow detection over a sufficiently wide frequency range Ω , and it has a high quality factor Q .

Now, we take the defect branch that corresponds to the region (b) of the previous Fig. 8, and we study the effect of the variation of d_0/D on the evolution of transmission and the quality factor. Fig. 9(a) shows that the transmission of the defect branch (a) in the previous figure is decreased with the increase d_0/D from 0.75 until 0.86; this shows that there is dissipation inside the defect branch (loss of energy of a defect branch), but from $d_0/D = 0.86$, the transmission starts to increase up to $d_0/D = 1$ where $T = 0.9743$, which shows that the dissipation inside the defect branch disappears in this defect length rang. Fig. 9(b) clearly shows that the quality factor is increased when d_0/D is varied between $d_0/D = 0.75$ and $d_0/D = 0.77$. This result displays that our defect branch is selective with a high quality factor $Q = 173$ when $d_0/D = 0.77$. After this value of defect length, the quality factor decreases with the increase of d_0/D and tends to $Q = 80$ for $d_0/D = 1$. This behavior is due to the increase of the width at half maximum of the transmission peaks.

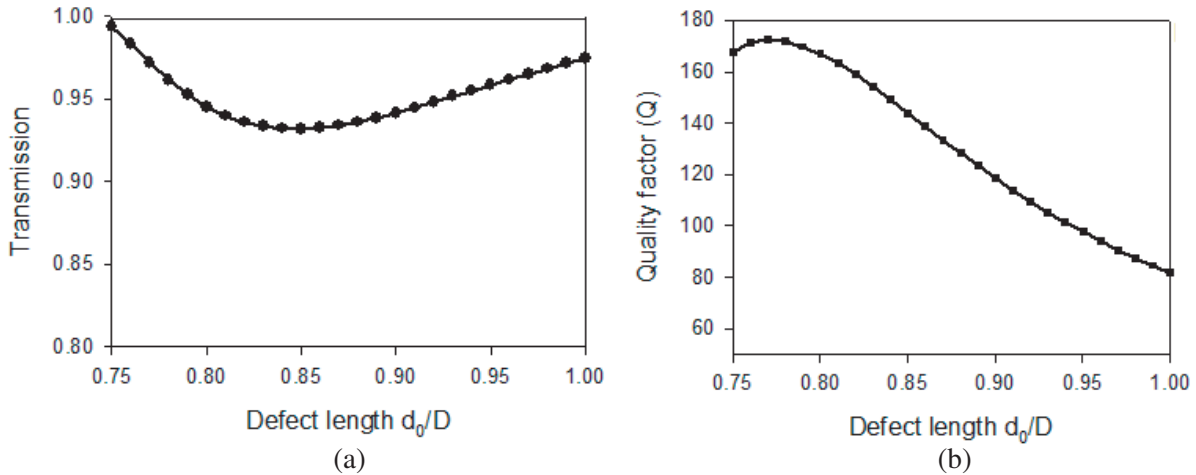


Figure 9. (a) represents the variation transmission for defect branches in area (a) in Fig. 8 as a function of the defect length d_0/D . (b) represents the variation of quality factor Q for these defect branches.

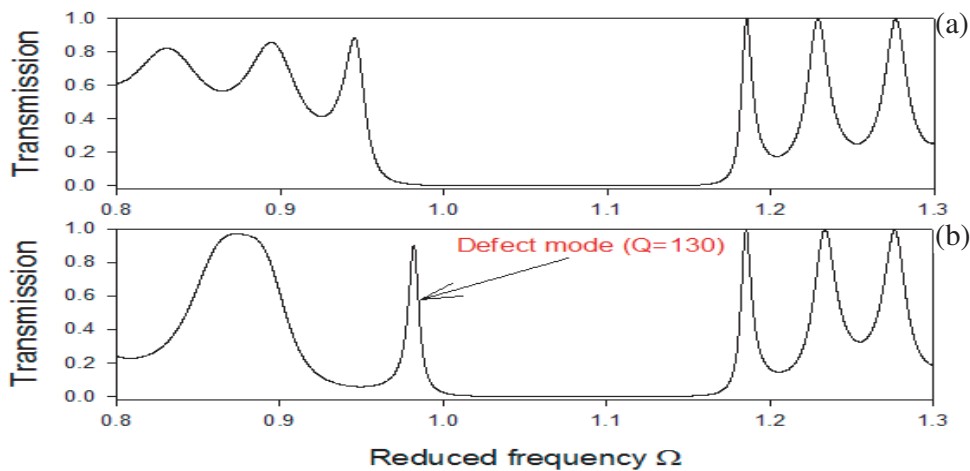


Figure 10. Transmission spectrum as a function of reduced frequency Ω when the structure is perfect (curve a) and when we create the defect at the lateral branch level (b) with $d_0/D = 0.25$, $N' = N'_0 = 1$, $N = 8$ and $J = 4$.

Due to the comb-like design and good coefficient of transmission and quality factor, these results demonstrate the potentiality of meta-material based filters in applications requiring wide band and ultra-wideband.

Also note that creating the defect inside the structure by using the boundary condition ($E = 0$) can obtain the defect modes inside the band gaps. This result is very clear in Fig. 10 when a defect mode exists around $\Omega = 0.98$ with their quality factor $Q = 130$.

In practical applications, one usually inclines to design a narrow filter with large band gaps which can modulate the defect mode in a larger frequency range with very high transmission and high quality factor. One could achieve this just by changing the defect length and/or the number of resonators grafted defect in each site.

4. CONCLUSION

Using the interface response theory, we have investigated the propagation of electromagnetic waves in 1D comb-like photonic structure. This comb-like structure is constituted by a periodicity of MNG segment and grafted in each site by a finite number of ENG resonators. The presence of resonators defect in these comb-like structure gives rise to localized modes (defect modes) inside the band gaps. These defect modes appear as peaks of high amplitude in the transmission spectrum. We have shown that the transmission of defect modes and their phase time is higher when the defect is located in the middle of the structure. Similarly, we find that the defect modes become very narrow when increasing the number of defect resonators grafted (the same thing for phase time). The transmission of these modes is diminished when the number of sites N is increased. The electromagnetic band structure shows that there are defect modes in a well-defined frequency range that decreases as the defect length increases, and their transmission and quality factor are very sensitive to the variation of defect length d_0/D .

ACKNOWLEDGMENT

We thank Profs. A. Mazari and M. Elachouri for their very critical comments to improve the English and the form of this article.

REFERENCES

1. Zhou, H., C. Wang, and H. Peng, "A novel double-incidence and multi-band left-handed metamaterials composed of double Z-shaped structure," *Journal of Materials Science: Materials in Electronics*, Vol. 27, 2534–2544, 2016.
2. Bi, K., J. Zhou, X. Liu, C. Lan, and H. Zhao, "Multi-band negative refractive index in ferrite-based metamaterials," *Progress In Electromagnetic Research*, Vol. 140, 457–469, 2013.
3. Li, J., F.-Q. Yang, and J. F. Dong, "Design and simulation of L-shaped chiral negative refractive index structure," *Progress In Electromagnetic Research*, Vol. 116, 395–408, 2011.
4. Cao, T. and M. J. Cryan, "Modeling of optical trapping using double negative index fishnet metamaterials," *Progress In Electromagnetic Research*, Vol. 129, 33–49, 2012.
5. Zhu, W., I. D. Rukhlenko, and M. Premaratne, "Maneuvering propagation of surface plasmon polaritons using complementary medium inserts," *IEEE Photonics Journal*, Vol. 4, No. 3, 741–747, 2012.
6. Zhu, J. H., S. Y. Wei, N. Haldolaarachchige, J. He, D. P. Young, and Z. H. Guo, "Very large magnetoresistive graphene disk with negative permittivity," *Nanoscale*, Vol. 4, 152–156, 2012.
7. Cheng, Y., Y. Nie, and R. Z. Gong, "Giant optical activity and negative refractive index using complementary U-shaped structure assembly," *Progress In Electromagnetic Research M*, Vol. 25, 239–253, 2012.
8. Zeng, R., Y. Yang, and S. Zhu, "Casimir force between anisotropic single-negative metamaterials," *Physical Review A*, Vol. 87, 063823–063829, 2013.

9. Xu, H. X., G. M. Wang, M. Q. Qi, and H. Y. Zeng, "Ultra-small single-negative electric metamaterials for electromagnetic coupling reduction of microstrip antenna array," *Optics Express*, Vol. 20, 21968–21976, 2012.
10. Alu, A. and N. Engheta, "Pairing an epsilon-negative slab with a mu-negative slab: Resonance, tunneling and transparency," *IEEE Transactions on Antennas and Propagation*, Vol. 51, 2558–2571, 2003.
11. Dhouibi, A., S. N. Burokur, A. Lustrac, and A. Priou, "Comparison of compact electric-LC resonators for negative permittivity metamaterials," *Microwave and Optical Technology Letters*, Vol. 54, 2287–2295, 2012.
12. Sun, K., P. Xie, Z. Wang, T. Su, Q. Shao, J. Ryu, X. Zhang, J. Guo, A. Shankar, J. Li, R. Fan, D. Cao, and Z. Guo, "Flexible polydimethylsiloxane/multi-walled carbon nanotubes membranous metamaterials with negative permittivity," *Polymer*, Vol. 125, 50–57, 2017.
13. Naqui, J. and F. Martin, "Angular displacement and velocity sensors based on electric-LC (ELC) loaded microstrip lines," *IEEE Sensors Journal*, Vol. 14, No. 4, 939–940, 2014.
14. Rawat, V., V. Nadkarni, and S. N. Kale, "Band flex fuel sensor using electrical metamaterial device," *Applied Physics A*, Vol. 123, 75–78, 2017.
15. Khan, O. M., Z. U. Islam, Q. U. Islam, and F. A. Bhatti, "Multiband high-gain printed yagi array using square spiral ring metamaterial structures for S-band applications," *IEEE Antennas and Wireless Propagation Letters*, Vol. 13, 1100–1103, 2014.
16. Xu, X., Y. Li, and X. Miao, "Robust waveguide against surface perturbations due to band inversion in two kinds of single-negative metamaterials," *Europhysics Letters*, Vol. 116, 44001–44007, 2016.
17. Jiang, H., H. Chen, and Y. E. Zhang, "Properties of one-dimensional photonic crystals containing single-negative materials," *Physics Letters E*, Vol. 69, 066607–066612, 2004.
18. Wang, L.-G., H. Chen, and S. Y. Zhu, "Omnidirectional gap and defect mode of one-dimensional photonic crystals with single-negative materials," *Physical Review B*, Vol. 70, 245102–245107, 2004.
19. Mackay, T. G., "Towards metamaterials with giant dielectric anisotropy via homogenization: An analytical study," *Photonics and Nanostructures — Fundamentals and Applications*, Vol. 13, 8–19, 2015.
20. Mikhaylovskiy, R. V., E. Hendry, and V. V. Kruglyak, "Negative permeability due to exchange spin-wave resonances in thin magnetic films with surface pinning," *Physical Review*, Vol. 82, 195446–195455, 2010.
21. Thibaudau, P. and J. Tranchida, "Frequency-dependent effective permeability tensor of unsaturated polycrystalline ferrites," *Journal of Physics: Applied Physics*, Vol. 118, 053901–053901, 2015.
22. Thapaa, K. B., P. C. Pandey, P. P. Singhc, and S. P. Ojha, "Tunable characteristics of one dimensional magnetic photonic crystal composed with single-negative materials," *Optik*, Vol. 124, 6631–6635, 2013.
23. Marathe, D. and K. Kulat, "A compact triple-band negative permittivity metamaterial for C, X-band applications," *International Journal of Antennas and Propagation*, Vol. 2017, 1–13, 2017.
24. Faruque, I. S. S., M. R. Iqbal, and M. T. Islam, "A New SNG metamaterial for S-band microwave applications," *Journal of Electrical & Electronics Engineering*, Vol. 7, 13–16, 2014.
25. Vasseur, J. O., P. A. Deymier, L. Dolorzynski, B. Djafari-Rouhani, and A. Akjouj, "Absolute band gaps and electromagnetic transmission in quasi-one-dimensional comb structures," *Physical Review B*, Vol. 55, 10434–10442, 1997.
26. Srivastava, S. K. and S. P. Ojha, "Enlarged photonic band gaps in one-dimensional magnetic star waveguide structure," *Progress In Electromagnetic Research M*, Vol. 9, 21–34, 2009.
27. Ben-Ali, Y., Z. Tahri, A. Ouariach, and D. Bria, "Double frequency filtering by photonic comb-like," *IEEE Xplore*, 1–6, 2019.
28. Vasseur, J. O., P. A. Deymier, L. Dolorzynski, B. Djafari-Rouhani, and A. Akjouj, "Defect modes in one-dimensional comblike photonic waveguides," *Physical Review B*, 13446–13452, 1999.
29. Cocolozzi, G. H., L. Dobrzynski, B. Djafari-Rouhani, H. Al-Wahsh, and D. Bria, "Electromagnetic wave propagation in quasi-one-dimensional comb-like structures made up of dissipative negative-

- phase-velocity materials,” *Journal of Physics: Condensed Matter*, Vol. 18, 3683–3690, 2006.
30. Yin, C. P. and H. Z. Wang, “Narrow transmission bands of quasi-1D comb-like photonic waveguides containing negative index materials,” *Physics Letters A*, Vol. 373, 1093–1096, 2009.
 31. Weng, Y., Z. G. Wang, and H. Chen, “Band structure of comb-like photonic crystals containing meta-materials,” *Optics Communications*, Vol. 277, 80–83, 2007.
 32. Zhang, L., Z. Wang, H. Chen, H. Li, and Y. Zhang, “Experimental study of quasi-one-dimensional comb-like photonic crystals containing left-handed material,” *Optics Communications*, Vol. 281, 3681–3685, 2008.
 33. Tan, W., Y. Sun, Z. G. Wang, and H. Chen, “Propagation of photons in metallic chain through side-branch resonators,” *Journal of Physics D: Applied Physics*, Vol. 44, 335101–335101, 2011.
 34. Tan, W., Z. Wang, and H. Chen, “Complete tuning of light through mu-negative media,” *Progress In Electromagnetic Research M*, Vol. 8, 27–37, 2009.
 35. Ben-Ali, Y., Z. Tahri, F. Falyouni, and D. Bria, “Study about a filter using a resonator defect in a one-dimensional photonic comb containing a left-hand material,” *Proceedings of the 1st International Conference on Electronic Engineering and Renewable Energy, ICEERE*, Saidia, 2018.
 36. Fang, W., Y. Z. Cheng, X. Wang, Y. N. Zhang, Y. Nie, and R. Z. Gong, “Narrow band filter at 1550 nm based on quasi-one-dimensional photonic crystal with a mirror-symmetric heterostructure,” *Materials*, Vol. 11, 1099–1108, 2018.
 37. Wang, F., Y. Z. Cheng, X. Wang, D. Qi, H. Luo, and R. Z. Gong, “Effective modulation of the photonic band gap based on Ge/ZnS one dimensional photonic crystal at the infrared band,” *Optical Materials*, Vol. 75, 373–378, 2018.
 38. Vasseur, J. O., P. A. Deymier, L. Dolorzynski, B. Djafari-Rouhani, and A. Akjouj, “Defect modes in one-dimensional comblike photonic waveguides,” *Physical Review*, Vol. 59, 13446–13452, 1999.
 39. Ben-Ali, Y., Z. Tahri, A. Bouzidi, D. Bria, A. Khettabi, and A. Nougouai, “Propagation of electromagnetic waves in a one-dimensional photonic crystal containing two defects,” *Journal of Materials and Environmental Sciences*, Vol. 8, 870–876, 2017.